698 *Bull. Chem. Soc. Jpn. Vol. 86, No. 6, 698–706 (2013)* *© 2013 The Chemical Society of Japan*

Selected Papers

A Redox-Active, Amphoteric Pyrogallolaldehyde Derivative: Electrochemical Characterization and Schiff Base Formation for Constructing Multifunctional Salphen Complexes

Hajime Shingai, Hirohiko Houjou,* Isao Yoshikawa, and Koji Araki

Institute of Industrial Science, The University of Tokyo, 4-6-1 Komaba, Meguro-ku, Tokyo 153-8505

Received November 13, 2012; E-mail: houjou@iis.u-tokyo.ac.jp

We synthesized and determined the crystal structure of a novel pyrogallolaldehyde derivative with a 5-dimethylaminomethyl group. In solution, this compound underwent autoxidation to form unidentified blue species under ambient conditions. Electrochemical measurements revealed that addition of a base promoted the autoxidation, whereas addition of an acid effectively suppressed it. Using *p*-toluenesulfonic acid, we isolated a hydroxy-rich salphen-type Schiff base ligand as an ammonium salt of the acid. We obtained several transition-metal complexes of this ligand that retained its antioxidant stability. We discuss the spectroscopic and electrochemical properties of these complexes in comparison with analogous complexes without a 5-dimethylaminomethyl group.

The electrochemistry of phenoxy-bearing compounds is of considerable importance for understanding biological catalytic systems like ribonucleotide reductase,[1] galactose oxidase,[2] and glyoxal oxidase.[3] The phenoxyl radical and its complexes with metals play an important role in the action of these enzymes, and numerous complexes have been proposed as models for the enzyme active sites.[4–9] Those model complexes exhibit interesting electrochemical phenomenon of valence tautomerism, or redox isomerism,[10–13] by virtue of a fascinating interplay between ligand-centered and metal-centered radical states. The complexes with redox-active ligands have also received attention because of their potential applications for nonlinear optical materials,[14] electroconductive materials,[15] and chromotropic materials,[16] the properties of which can be controlled by various external stimuli. Because the stability of the oxidized species depends on the electron-donating character of ligands, an hydroxy-rich aromatic core like pyrogallol is a good candidate for the component of redox-active ligands.

Recently, transition-metal complexes of Schiff base ligands, including salen (salenH_2: *N*,*N*′-disalicylideneethylenediamine) and salphen (salphenH_2: *N*,*N*′-disalicylidene-*o*-phenylenediamine), have been extensively studied with a focus on the above-mentioned properties related to valence tautomerism.[17–20] Also, there have been several attempts to take advantage of the radical-generating ability of hydroxy-rich salicylaldiminato complexes to develop artificial nucleases.[21,22] Hydroxy-rich salens or salphens would also provide access to various metallosupramolecular systems and metal-containing materials.[23–25] Several macrocyclic complexes composed of pyrocatechualdehyde (2,3-dihydroxybenzaldehyde) and pyrogallolaldehyde (2,3,4-trihydroxybenzaldehyde) have been reported to capture metal ions or guest molecules, resulting in fascinating multicomponent systems.[26–28] In view of the potential importance of complexes with redox-active ligand(s), developing a new component molecule for constructing multinuclear, stimulus-responsive materials is a worthwhile challenge. For this purpose, the coordination chemistry and redox activity of the multifunctional ligand must be controlled.

To design a new redox-active pyrogallol derivative as a component of salen/salphen ligands, we noted an interesting concerted proton–electron-transfer protocol, by which the resultant phenoxyl radical would be stabilized with a proximal ammonium/iminium hydrogen.[29–31] In this study, we synthesized a pyrogallolaldehyde bearing an ammonium hydrogen in the proximity of its phenol group as a prototype multifunctional ligand, and here we describe its electrochemical characterization, Schiff base formation, and subsequent metal-complexation.

Results and Discussion

Structure and Properties of the Aldehyde $1H_3$. A Mannich reaction of pyrogallolaldehyde afforded the corresponding 5-(*N*,*N*′-dimethylaminomethyl) derivative $\mathbf{1H_3}$ in good yield (Scheme 1). The 1-formyl group of $\mathbf{1H_3}$ is relatively inert, so undesired polymerization did not occur. Compound $\mathbf{1H_3}$ was recrystallized from a THF–water system to give a single crystal of X-ray quality. Interestingly, the melting point

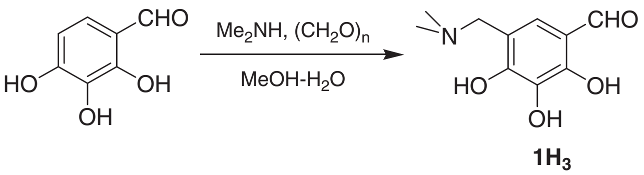

$\mathbf{1H_3}$

Scheme 1. Preparation of 2,3,4-trihydroxy-5-dimethylaminomethylbenzaldehyde ($\mathbf{1H_3}$).

Published on the web June 15, 2013; doi:10.1246/bcsj.20120316

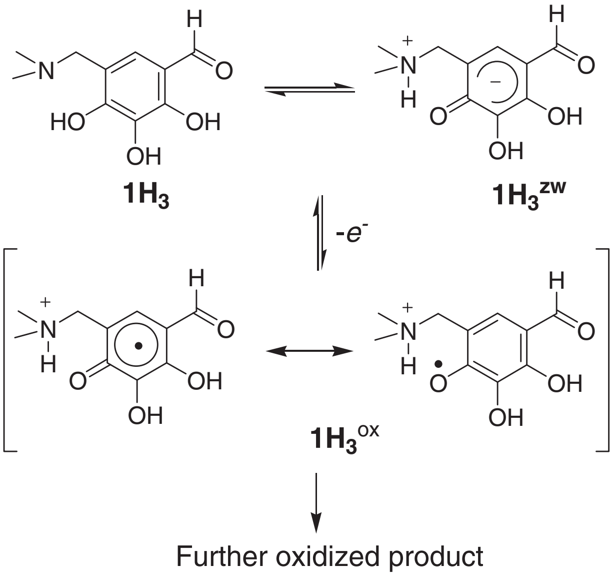

Scheme 2. A presumptive reaction scheme for the autoxidization of **1H$_3$**.

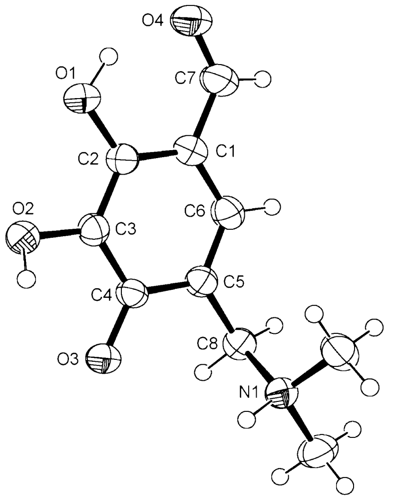

Figure 1. ORTEP drawing of **1H$_3$**. One of two asymmetric units is shown, and a water molecule is omitted for clarity. The atoms are numbered for comparison with the structural data listed in Table 1.

Table 1. Selected Bond Length[a] (Å) and HOMA Indexes Derived from the Crystal Structures of **1H$_3$** and Pyrogallolaldehyde

Bond	Unit 1	Unit 2	Pyrogallolaldehyde[b]
C1–C2	1.417(4)	1.406(4)	1.418
C2–C3	1.379(4)	1.373(4)	1.375
C3–C4	1.424(4)	1.432(4)	1.399
C4–C5	1.435(4)	1.434(4)	1.396
C5–C6	1.373(4)	1.369(4)	1.373
C6–C1	1.400(4)	1.410(4)	1.405
C1–C7	1.430(4)	1.426(5)	1.426
C2–O1	1.362(4)	1.360(4)	1.355
C3–O2	1.368(3)	1.371(3)	1.368
C4–O3	1.283(3)	1.284(3)	1.356
HOMA[c]	0.790	0.767	0.905, 0.938

a) Standard deviations in parentheses. b) From Ref. 32. Bond lengths are averaged over two asymmetric units in the crystal. c) $\text{HOMA} = 1 - \frac{\alpha}{n}\sum_{i=1}^{n}(R_{\text{opt}} - R_i)^2$, where $\alpha = 257.7$, and $R_{\text{opt}} = 1.388$, as defined in Ref. 33.

of the crystalline sample (159–160 °C) was higher than that of the as-prepared sample (146–147 °C) even though the ^{1}H NMR spectra of the two samples were identical to each other. Furthermore, the IR spectrum of the recrystallized sample was much different from that of the as-prepared sample (Figure S1, Supporting Information), probably owing to differences in hydrogen bonding and dissociation state. Analysis of the crystal structure suggested that the proton of the 4-hydroxy group was dissociated and that the nitrogen atom was protonated (hereafter referred to as **1H$_3$$^{\text{zw}}$**, also shown in Scheme 2, vide infra). Figure 1 shows the ORTEP drawing of one of the two independent asymmetric units, and Table 1 lists selected bond lengths. In both asymmetric units, the C4–O3 distances (1.283 and 1.284 Å) were markedly shorter than the corresponding distance (1.356 Å) in pyrogallolaldehyde.[32] Additionally, introduction of the 5-dimethylaminomethyl group lengthened the C3–C4 distances (1.424 and 1.432 Å) and the C4–C5 distances (1.435 and 1.434 Å) as compared to the corresponding distances (1.399 and 1.396 Å, respectively) in pyrogallolaldehyde. We evaluated the overall distortion of the benzene ring by means of the harmonic oscillator model for aromaticity (HOMA) index,[33] a geometry-based criterion of aromaticity. The relatively low HOMA values (0.790 and 0.767) indicated a loss of aromaticity, suggesting that the C4–O3 bond of **1H$_3$$^{\text{zw}}$** assumed keto-like character;[34] therefore, the negative charge was delocalized over the benzene ring. Mulliken population analysis (by Hartree–Fock/6-311G** level of calculation) showed that on going from **1H$_3$** to **1H$_3$$^{\text{zw}}$**, the net charge at 4-O(H) group changes by −0.556*e*, while that at 5-CH$_2$N(H)(CH$_3$)$_2$ group changes by +0.689*e*. The difference negative charge (−0.134*e*) was found distributed over the benzene ring, especially at the carbon C5 (−0.110*e*), and the formyl group (−0.048*e*) (for detail, Table S1). These changes in electronic distribution are reasonably in agreement with prediction from resonance structures. As for packing structure, the asymmetric units formed a cyclic tetramer in which the protonated amino groups, 3-OH groups, and 4-O groups were connected through multiple hydrogen bonds (Figure 2). A water molecule, though it was considerably disordered, was found at every site where one cyclic tetramer was connected with another (Figure S2, Supporting Information).

The crystal of **1H$_3$** was colorless to pale yellow, but a DMF solution of the crystal rapidly turned blue under atmospheric conditions. The UV–vis spectra of **1H$_3$** in DMF showed a broad absorption band around 600–700 nm (Figure 3). The absorbance at 600 nm initially increased with time but began to diminish gradually after 90 min (Figure 3, inset). In contrast, the absorbance at 400 nm increased monotonically, and as a result, the solution gradually turned yellow. Interestingly, an aqueous solution of **1H$_3$** was yellow from the beginning, whereas a THF solution was almost colorless and remained so throughout the time course of the experiment. Taking into

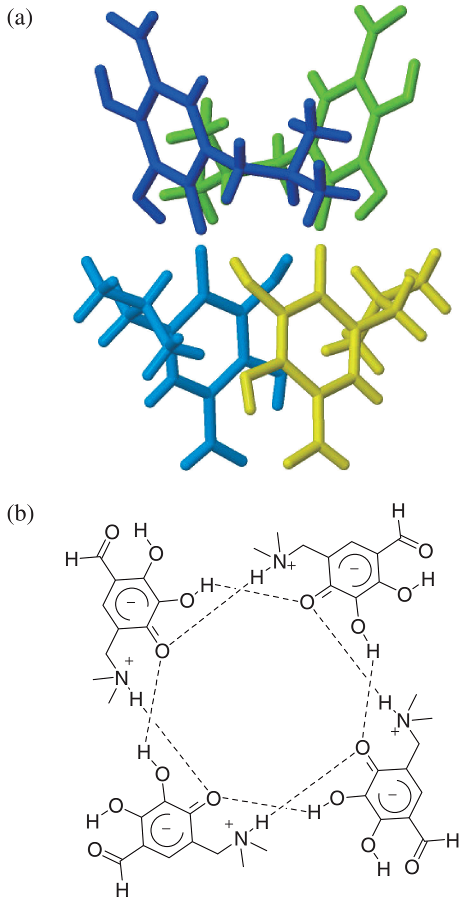

Figure 2. Hydrogen-bonding network in the cyclic tetramer of $\mathbf{1H_3}^{zw}$; (a) stick model representation of the crystal structure, and (b) drawing for showing topological relation.

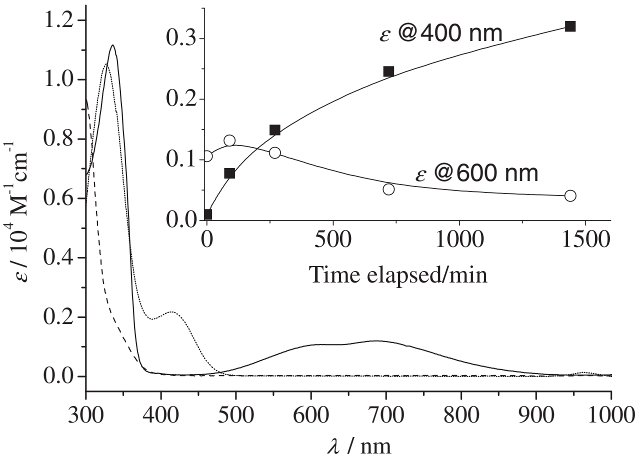

Figure 3. UV–vis spectra of $\mathbf{1H_3}$ in DMF (solid line), water (dotted line), and THF (dashed line). The inset shows the time dependence of the absorptivity (ε) of the DMF solution.

account the results for some solvents (DMSO, acetonitrile, methanol, and ethanol), we can summarize the solvent-dependence that aprotic polar solvents promote the formation of the blue species, while aquaous environment lead to another path of reaction.

These spectroscopic results imply that $\mathbf{1H_3}$ easily underwent autoxidation in solution to give the blue species. We confirmed that the characteristic absorption at 600–700 nm was intensified associatively with bulk electrolysis or addition of appropriate oxidation reagents (Figures S4a and S4b). Although the spectral features imply the presence of a phenoxy radical,[7c,29,35,36] we could not detect any significant ESR signals after the efforts of preparation under various conditions (e.g., in acetonitrile with ferrocenium hexafluorophosphate at 77 K, 210K) (Figure S4c). For the moment, we have not been able to identify the blue species: while one candidate is a semiquinone radical that is rapidly decomposed or undergoes further oxidation to form a product such as an imine or orthoquinone,[37] there is some room for discussion about charge-transfer complexes or some spin-coupled diamagnetic species. The formation of the blue species was accelerated appreciably by the addition of one equivalent of triethylamine, whereas the initial increase of the absorption at 600 nm was suppressed by the addition of *p*-toluene sulfonic acid (Figure S3, Supporting Information). These results indicate that the progress of these reactions was closely coupled with the association and dissociation of protons. The proposed reaction scheme is given in Scheme 2.

Among the ^{1}H NMR signals of $\mathbf{1H_3}$ (in DMSO-d_6), we particularly noted three singlets (3.75, 6.92, and 9.59 ppm), which were assigned to methylene, aromatic, and formyl protons, respectively; these peaks were shifted to 4.21, 7.36, and 9.86 ppm, respectively, by the addition of *p*-toluenesulfonic acid (Figure S5, Supporting Information). The substantial change in the chemical shift of the methylene protons indicates protonation of the $-N(CH_3)_2$ group, and the downfield shift of the protons in the aromatic region indicates suppression of deprotonation of the 4-OH group. In contrast, the addition of triethylamine resulted in only minor changes in the chemical shifts of these protons (to 3.70, 6.89, and 9.55 ppm) relative to the shifts under neutral conditions. The chemical shifts measured in D_2O were 4.14, 7.07, and 9.59 ppm, implying the protonation of the amino group, even taking solvent difference into account. These results suggest that in a polar solvent, $\mathbf{1H_3}$ was in equilibrium with its zwitterionic form $\mathbf{1H_3}^{zw}$ (Scheme 2).

The cyclic voltammogram of $\mathbf{1H_3}$ in DMF exhibited several irreversible peaks in the region of −1000 to +1000 mV (vs. Ag^+/Ag) (Figure 4). The intense anodic peak at 620 mV was similar to that observed in the voltammogram of pyrogallolaldehyde (Figure S6). As is the case for other phenols, the oxidation corresponding to this peak was irreversible, probably owing to deprotonation of the oxidized form.[29] The deprotonated form of pyrogallolaldehyde was reduced at 0 and −350 mV, but the corresponding peak (−330 mV) for $\mathbf{1H_3}$ was negligibly small. Instead, a new cathodic peak and a new anodic peak appeared at −820 mV and around −140 mV, respectively, both of which had a similar current magnitude. Upon stepwise addition of triethylamine, the anodic peak at −140 mV developed (Figure 4). A similar phenomenon was observed for pyrogallolaldehyde (Figure S6). The anodic peak grew with appearance of a new peak at 350 mV, becoming saturated after the addition of 2 equiv of amine (see inset). This result suggests that this peak overlapped with the oxidation waves of the 4-dissociated form $\mathbf{1H_3}^{zw}$ and the 3,4-doubly-dissociated form

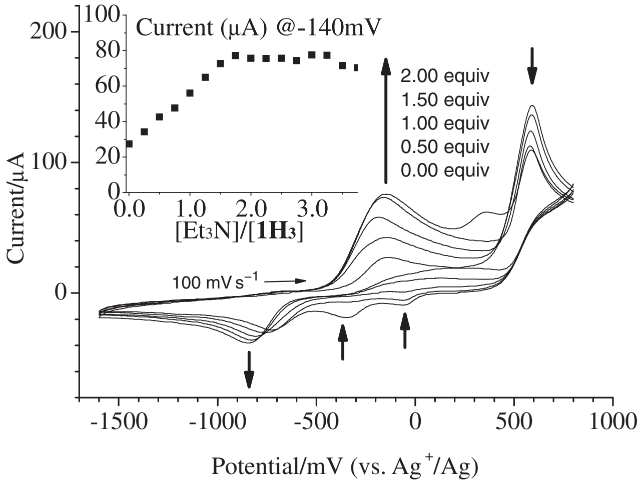

Figure 4. Cyclic voltammograms of $1H_3$ with stepwise addition of triethylamine.

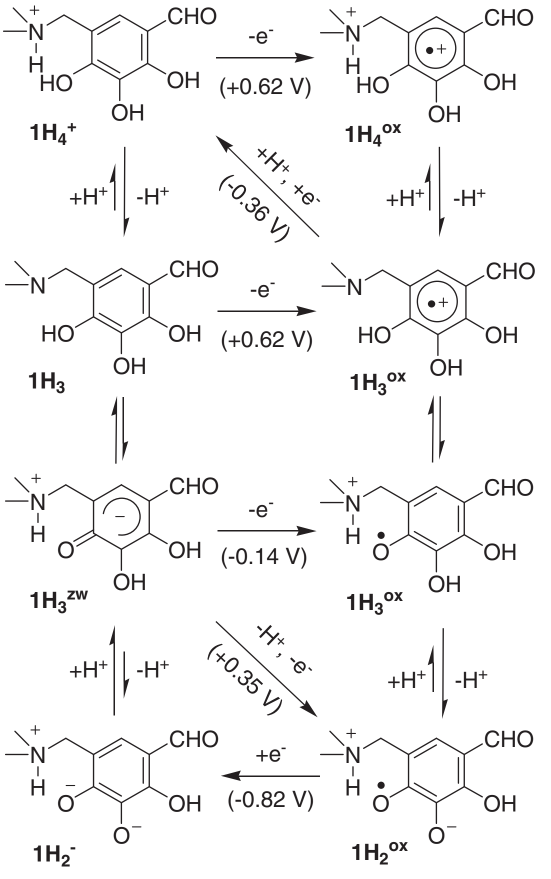

Scheme 3. Plausible redox scheme for $1H_3$.

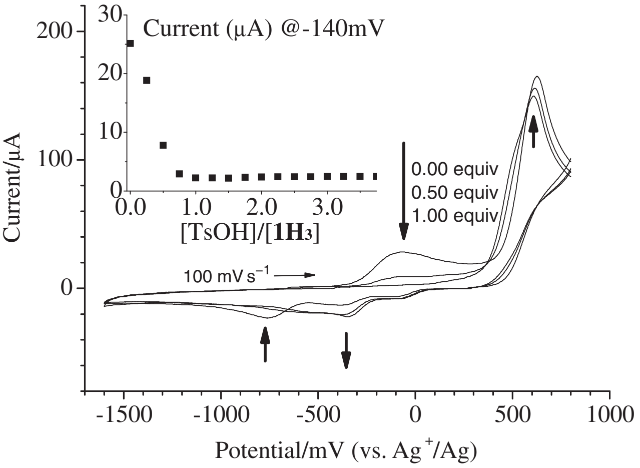

Figure 5. Cyclic voltammograms of $1H_3$ with addition of various amounts of *p*-toluenesulfonic acid.

$1H_2^-$ (for plausible structures, Scheme 3). Along with this change, the anodic current at 620 mV diminished and the cathodic current at −820 mV increased upon addition of the amine, in agreement with the above interpretation.

In contrast, upon stepwise addition of *p*-toluenesulfonic acid, the anodic peak at −140 mV gradually diminished (Figure 5). The change in the anodic current became saturated after the addition of 1 equiv of acid (see inset), suggesting that protonation of the –N(CH_3)$_2$ group suppressed the generation of $1H_3^{ox}$ at this potential. Along with this change, the cathodic peak at −820 mV gradually diminished, and another cathodic peak developed at −360 mV. Like the cathodic peak at −350 mV of pyrogallolaldehyde, the latter peak appears to correspond to reduction of the deprotonated semiquinone (or its proton-transferred form). As a result, the profile of the cyclic voltammogram of $1H_3$ became quite similar to that of pyrogallolaldehyde when at least 1 equiv of acid was added.

On the basis of the above-mentioned results, we assumed the proton-coupled redox scheme for $1H_3$ shown in Scheme 3. Note that the structures of deprotonated forms have not been unambiguously determined, because there are several possible dissociation states of the 2-OH, 3-OH, 4-OH, and 5-$CH_2NH^+(CH_3)_2$ groups. At this stage, we can safely conclude that under neutral to basic conditions, $1H_3$ underwent facile oxidation to $1H_3^{ox}$. The oxidized species underwent further oxidation, coupled with proton dissociation, resulting in considerable irreversibility in the cyclic voltammogram. The electrochemical measurements indicate that the addition of 1 equiv of acid markedly stabilized $1H_3$ against oxidation; these measurements were in agreement with the UV–vis results. Scheme 3 was also validated by means of a series of cyclic voltammetry experiments in selected scan ranges (Figure S7, Supporting Information). Unless the potential exceeded +200 mV, the reduction peak at −360 mV did not appear. These experiments also confirmed that the oxidation peak at +40 mV and the reduction peak at −820 mV were coupled with each other.

Schiff Base Ligand and Its Complexes. The reaction of pyrogallolaldehyde with 4,5-dimethylphenylenediamine afforded the 3,3′,4,4′-tetrahydroxy derivative of the salphen ligand (H_2L^b) in high yield (Scheme 4). However, a similar reaction of $1H_3$ in chloroform–methanol (v/v = 1/1) resulted in dark brown sticky material, in which we did not detect any trace of the desired product. Use of nitrogen-bubbled solvents significantly suppressed the generation of unidentifiable byproducts. In view of the above discussion, we suggest that in the presence of molecular oxygen $1H_3$ underwent irreversible oxidation owing to the basicity of the phenylenediamine, and hence no Schiff base product was formed. When we performed

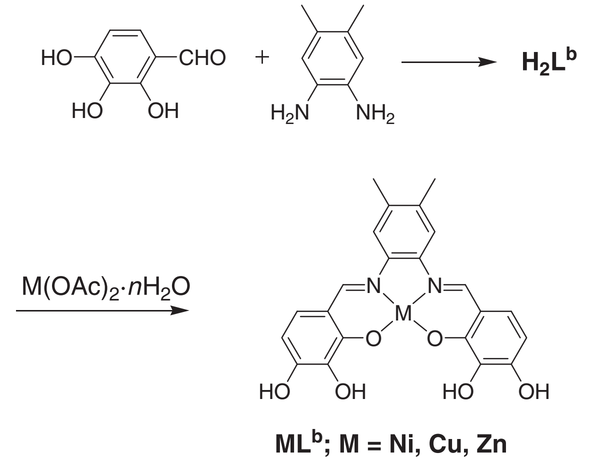

Scheme 4. Synthesis of a pyrogallol-derived salphen ligand and its metal complex.

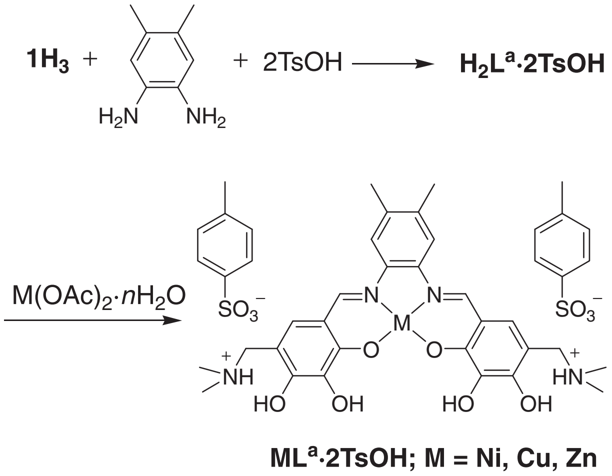

Scheme 5. Synthesis of a functionalized salphen ligand and its metal complex.

the same reaction in the presence of 1 equiv of *p*-toluenesulfonic acid with respect to **$1H_3$**, we obtained the 3,3′,4,4′-tetrahydroxy-5,5′-bis(*N*,*N*-dimethylaminomethyl) derivative of salphen in 95% yield as its di-*p*-toluenesulfonic acid salt ($H_2L^a \cdot 2TsOH$, Scheme 5). The ^1H NMR chemical shift of the methylene protons was 4.18 ppm, which indicates that the amino group was protonated, like that of **$1H_4^+$**.

The functionalized salphen ligand $H_2L^a \cdot 2TsOH$ was allowed to react separately with the acetates of nickel(II), copper(II), and zinc(II). The reaction mixtures readily afforded crystalline $NiL^a \cdot 2TsOH$, $CuL^a \cdot 2TsOH$, and $ZnL^a \cdot 2TsOH$, respectively, in good yields. The ^1H NMR chemical shifts of the methylene ($-CH_2N(CH_3)_2$) protons were 4.14 ppm for the nickel complex and 4.12 ppm for the zinc complex, showing that these complexes also existed in protonated form in solution. There were two extremely broadened signals at 9.1 and 10.1 ppm for the nickel complex and at 9.0 and 10.0 ppm for the zinc complex. The peak areas indicated two protons for each peak, and the peaks were assignable to either 4-OH or –NH protons. Then, singlet peak at 8.75 ppm is attributable to 3-OH. When an additional 2 equiv of *p*-toluenesulfonic acid was added to $NiL^a \cdot 2TsOH$, the signal at 10.1 ppm became a sharp singlet, and the signal at 9.1 ppm sharpened as well (Figure 6). Upon addition of acid, the *N*-methylene and *N*-methyl protons appeared as doublets with coupling constants of 5.4–5.5 Hz, suggesting that the –NH signal appeared as a complicated multiplet if the proton was firmly associated with the amino group. Therefore, we assigned the broad signals at around 9 ppm observed for the nickel and zinc complexes to –NH protons. Relatively sharp singlets at 8.75 ppm for the nickel complex and at 7.86 ppm for the zinc complex were assigned to 3-OH protons; the sharpness of these peaks may have resulted from intramolecular hydrogen bonding to the O–(Ni or Zn) moiety. The corresponding peaks were observed at 9.36 ppm for NiL^b and at 9.12 ppm for ZnL^b. The chemical shift differences between the complexes of the two metals may have resulted from differences in the acidity of the OH groups. Although these assignments are tentative, the acceptable consistency of the spectra with the proposed salphen complex shows that there was no trace of any by-products formed by undesired coordination at the 3-OH or 4-OH group.

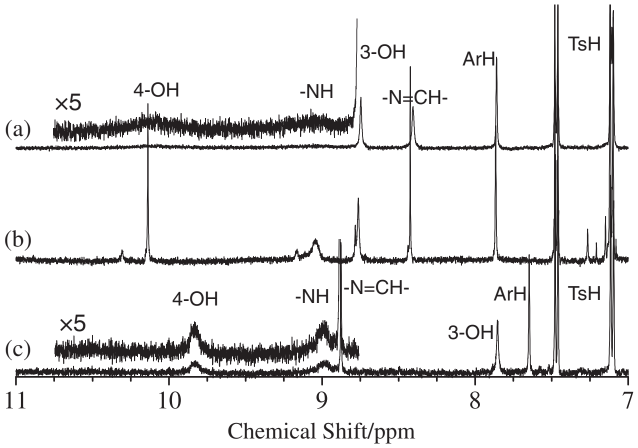

Figure 6. ^1H NMR spectra of functionalized salphen complexes: (a) $NiL^a \cdot 2TsOH$, (b) $NiL^a \cdot 2TsOH$ and additional 2 equiv of *p*-toluenesulfonic acid, and (c) $ZnL^a \cdot 2TsOH$.

The UV–vis spectra of $NiL^a \cdot 2TsOH$, $CuL^a \cdot 2TsOH$, and $ZnL^a \cdot 2TsOH$ were compared with the spectra of the corresponding NiL^b, CuL^b, and ZnL^b complexes (Figure 7). Note that 2 equiv of *p*-toluenesulfonic acid was added to the latter complexes to achieve dissociation states similar to those of the former. The spectral profiles of $ML^a \cdot 2TsOH$ and ML^b were quite similar to each other for all three sets of complexes, indicating that the electronic states of these complexes were essentially identical. However, the intensities of the shoulder bands (ca. 480 nm for nickel, ca. 460 nm for copper, and ca. 450 nm for zinc) at the low-energy absorption edge were slightly higher for the ML^a complexes. We attributed these bands to π–π^* transitions, mainly in the hydroxybenzaldehyde moieties; to some extent, these bands assumed the character of metal-to-ligand charge-transfer bands.[38] Thus, it is conceivable that slight modification of the acidity of the OH groups by the $-CH_2N^+H(CH_3)_2$ group was responsible for the changes in the spectra.

To investigate the spectroscopic and electrochemical properties of the metal complexes in their neutral states (ML^a), we added 2 equiv of triethylamine to the solutions of $ML^a \cdot 2TsOH$.

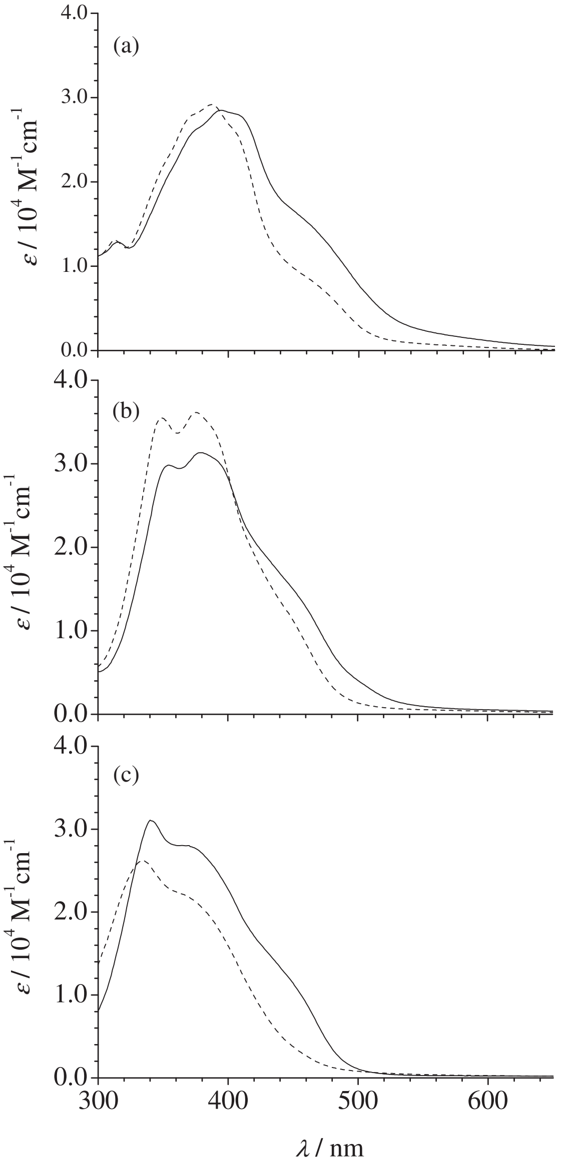

Figure 7. UV–vis spectra of ML^a•2TsOH (solid line) and ML^b (dashed line) complexes in DMSO with 2 equiv of acid: (a) M = Ni, (b) M = Cu, and (c) M = Zn.

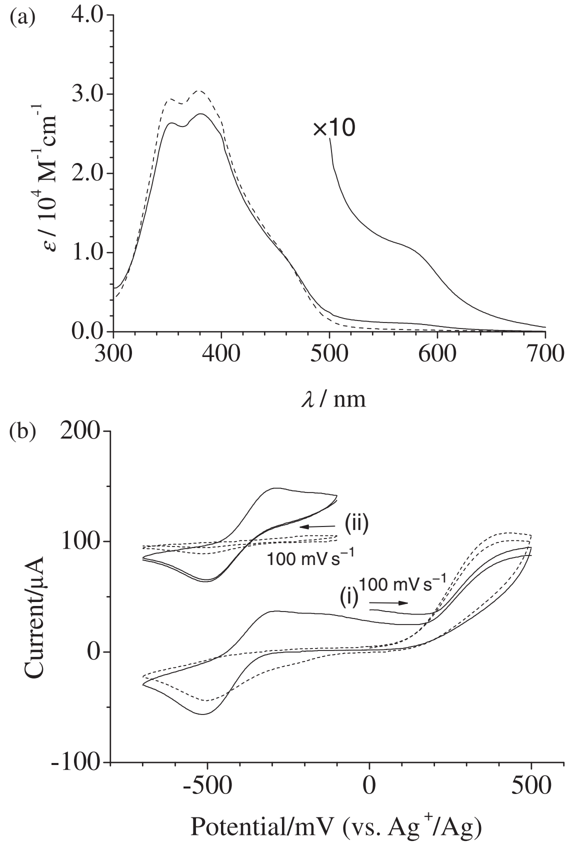

Figure 8. (a) UV–vis absorption spectra and (b) cyclic voltammograms of CuL^a•2TsOH before (dashed lines) and after (solid lines) the addition of triethylamine. In (b), scan regions were −700 to +500 mV for (i) and −700 to −100 mV for (ii). The baseline of voltammogram (ii) is shifted by +100 μA for clarity.

In the UV–vis absorption spectrum of CuL^a•2TsOH, the absorptivity of the peak at 580 nm increased slightly (to ca. 1000), whereas the absorptivity of the peak at 350–400 nm was slightly diminished (Figure 8a). These changes imply the formation of ligand-center oxidized species by autoxidation, as was observed for $\mathbf{1H_3}$ (Figure 3). Accordingly, we can assume that under neutral to basic conditions, CuL^a was easily oxidized. This assumption was supported by cyclic voltammograms (Figure 8b): under acidic conditions, we observed an oxidation wave at +400 mV and a reduction wave at −500 mV, whereas upon addition of triethylamine, a new oxidation wave appeared at −300 mV together with a slight decrease of the current at +400 mV. The peaks at −500 and −300 mV formed a pseudoreversible redox wave, attributable to the reaction shown in Scheme 4. It is conceivable that these two peaks correspond to the peaks at −820 and −140 mV observed for $\mathbf{1H_3}$ (Figure 4), because replacing the 2-OH proton with a copper ion would have changed the redox potentials. In contrast, we observed no remarkable changes in the absorption spectra of NiL^a•2TsOH and ZnL^a•2TsOH solutions when 2 equiv of triethylamine was added. However, the cyclic voltammogram of NiL^a•2TsOH changed drastically upon addition of the amine, as was observed for the copper complex (Figure S8). Although ZnL^a•2TsOH gave a voltammogram similar to that of CuL^a•2TsOH, it did not show any pronounced change upon addition of base. At present, we have no clear explanation for the difference in redox behavior dependent on metal species. One possible hypothesis is that the redox potential of the metal ion affects the stability of the oxidized ligand moiety. This topic needs to be discussed with further experiments in the future.

Conclusion

In summary, we synthesized a new amphoteric pyrogallolaldehyde ($\mathbf{1H_3}$) and investigated its electrochemical properties. This aldehyde was redox active and underwent facile autoxidation. Protonation of the side chains switched off the redox activity and hence facilitated further reactions such as Schiff base formation and metal complexation. We demonstrated the preparation of functionalized salphen-type complexes of some transition metals, which had electronic states that were essentially identical to those of the analogous hydroxy-rich salphen complexes. It is notable that we could switch on the redox function of the salphen complex by removing the proton on the side chain, which enabled us to access some complexes with oxidation locus on the ligand. Furthermore, we have a broad choice of amines, including diamines and triamines having various linker moieties, with which we will be able to construct metallosupramolecules and metal-containing polymers.

Experimental

General. All chemicals and solvents were purchased from Tokyo Kasei Kogyo (TCI) and used without further purification. UV–vis absorption spectra were measured for a 2×10^{-5} M solution of each solute with a JASCO V-630 spectrophotometer. NMR spectra were recorded on a JEOL ECS-400 instrument (400 MHz for ^{1}H) for DMSO-d_6 solution. IR spectra were recorded with a JEOL FT/IR-420 instrument. Electrochemical measurements were performed by using a conventional three-electrode cell with a glassy carbon working electrode, a platinum wire electrode, and an Ag^+/Ag reference electrode. The samples were prepared as 5.0 mM solutions in dry dimethylformamide with 0.1 M tetrabutylammonium hexafluorophosphate as the supporting electrolyte. Cyclic voltammograms were run by using a BAS 100B/W system. Solutions were purged with nitrogen gas before each run. Melting points were determined with an optical microscope equipped with a Linkam LK-600 temperature-variable stage; the heating rate was $2\,K\,min^{-1}$.

Synthesis of 2,3,4-Trihydroxy-5-dimethylaminomethylbenzaldehyde (1H$_3$). To 30 mL of methanol was added 1.08 g of aqueous dimethylamine (50%) (12 mmol for dimethylamine) and 0.36 g of paraformaldehyde (12 mmol for CH_2O unit). The mixture was stirred at 70 °C to obtain clear solution, to which 1.54 g of 2,3,4-trihydroxybenzaldehyde (10 mmol) was added. After 30 min of heating, the reaction mixture was left at ambient temperature to grow colorless to pale yellow precipitate. The product was collected by filtration, and washed with methanol (1.54 g, 73%). Mp 146–147 °C; Anal. Calcd for $C_{10}H_{13}NO_4$ (211.22): C, 56.86; H, 6.20; N, 6.63%. Found: C, 57.25; H, 6.33; N, 6.61%. FAB MS(+): $m/z = 212.2$ (212.09 calcd for $M + H^+$); IR (KBr): 1643 cm^{-1} ($\nu_{C=O}$); ^{1}H NMR: δ 2.45 (s, –CH$_3$, 6H), 3.80 (s, –CH$_2$–, 2H), 6.8 (br, –OH), 6.92 (s, ArH, 1H), 9.59 (s, –CHO, 1H); ^{13}C NMR: δ 42.8, 59.7, 111.9, 113.2, 124.8, 132.1, 148.8, 160.1, 191.0.

Synthesis of *N*,*N′*-Bis(2,3,4-trihydroxy-5-dimethylaminomethylbenzylidene)-4,5-dimethyl-1,2-diaminobenzene Di-*p*-toluenesulfonic Acid Salt (H$_2$L^a·2TsOH). To a THF solution (20 mL) of **1** (2.11 g, 10 mmol) and *p*-toluenesulfonic acid (1.72 g, 10 mmol) was added 0.68 g (5 mmol) of 4,5-dimethyl-1,2-phenylenediamine. Then the mixture separated an orange oil, which later crystallized within several hours. The crystalline material was collected by filtration and washed with THF (4.10 g, 95%). Mp 135–136 °C; Anal. Calcd for $C_{42}H_{50}N_4O_{12}S_2 \cdot H_2O$ (884.30): C, 57.00; H, 5.92; N, 6.33%. Found: C, 57.09; H, 6.23; N, 6.21%. FAB MS(+): $m/z = 523.8$ (523.26 calcd for $H_2L^a + H^+$); IR (KBr): 1625 cm^{-1} ($\nu_{C=N}$), 1034, 1009, 818, 682, 567 cm^{-1} (TsO$^-$); ^{1}H NMR: δ 2.28 (s, Ts–CH$_3$, 6H), 2.30 (s, Ar–CH$_3$, 6H), 2.73 (s, N–CH$_3$, 12H), 4.18 (s, –CH$_2$–, 4H), 7.10 (d, $^3J = 7.8$ Hz, TsH, 4H), 7.15 (s, ArH, 2H), 7.26 (s, ArH, 2H), 7.47 (d, $^3J = 7.8$ Hz, TsH, 4H), 8.78 (s, –N=CH–, 2H), 9.2–10.2 (br, –OH/–NH, 4H), 13.86 (brs, –OH, 2H), residual –OH signal (for 2H) was not observed as a recognizable peak; ^{13}C NMR: δ 19.2, 20.8, 42.1, 55.3, 109.3, 112.1, 120.5, 125.6, 127.7, 128.2, 132.6, 136.0, 137.9, 138.3, 145.5, 153.7, 162.5.

Synthesis of *N*,*N′*-Bis(2,3,4-trihydroxybenzylidene)-4,5-dimethyl-1,2-diaminobenzene (H$_2$L$_b$). To a methanol solution (50 mL) of 3.09 g of 2,3,4-trihydroxybenzaldehyde (20 mmol) was added 1.36 g (10 mmol) of 4,5-dimethyl-1,2-phenylenediamine. Within several hours the mixture gave a yellow precipitate, which was collected by filtration and washed with methanol (3.66 g, 90%). Mp 200–201 °C; Anal. Calcd for $C_{22}H_{20}N_2O_6$ (408.40): C, 64.70; H, 4.94; N, 6.86%. Found: C, 64.12; H, 4.87; N, 6.81%. FAB MS(+) $m/z = 409.1$ (409.14 calcd for $M + H^+$); IR (KBr): 1631 cm^{-1} ($\nu_{C=N}$); ^{1}H NMR: δ 2.28 (s, –CH$_3$, 6H), 6.38 (d, $^3J = 8.5$ Hz, ArH, 2H), 6.93 (d, $^3J = 8.5$ Hz, ArH, 2H), 7.19 (s, ArH, 2H), 8.71 (s, –N=CH–, 2H), 9.12 (brs, –OH, 4H), 13.46 (brs, –OH, 2H); ^{13}C NMR: δ 19.1, 107.8, 112.7, 120.5, 124.1, 132.4, 135.4, 139.2, 150.3, 152.0, 162.8.

Synthesis of Divalent Metal Complexes of L^a (ML^a·2TsOH; M = Ni, Cu, Zn). To a methanol solution (10 mL) of H$_2$L^a·2TsOH (0.87 g, 1 mmol) was added a methanol solution (10 mL) of the corresponding metal acetate hydrate (1 mmol). Within several hours the mixture gave a precipitate, which was collected by filtration and washed with diethyl ether.

NiL^a·2TsOH: Reddish brown solid (0.67 g, 73%). Mp 226–227 °C; Anal. Calcd for $C_{42}H_{48}N_4NiO_{12}S_2 \cdot H_2O$ (941.69): C, 53.57; H, 5.35; N, 5.95%. Found: C, 53.60; H, 5.57; N, 5.84%. FAB MS(+) $m/z = 579.7$ (579.15 calcd for $NiL^a + H^+$); IR (KBr): $\nu = 1626$ cm^{-1} ($\nu_{C=N}$), 1035, 1011, 817, 685, 569 cm^{-1} (TsO$^-$); ^{1}H NMR: δ 2.28 (s, Ar–CH$_3$/Ts–CH$_3$, 12H), 2.74 (s, N–CH$_3$, 12H), 4.14 (s, –CH$_2$–, 4H), 7.11 (s, ArH, 2H), 7.11 (d, $^3J = 8.0$ Hz, TsH, 4H), 7.47 (d, $^3J = 8.0$ Hz, TsH, 4H), 7.86 (s, ArH, 2H), 8.41 (s, –N=CH–, 2H), 8.75 (s, –OH, 2H), 9.00 (br, –NH, 2H), 10.1 (br, –OH, 2H); ^{13}C NMR has not been obtained because no signals were found for a concentrated sample solution. For this concentrated sample, ^{1}H NMR spectra gave significantly broadened signals.

CuL^a·2TsOH: Reddish brown solid (0.78 g, 84%). Mp 184–185 °C; Anal. Calcd for $C_{42}H_{48}CuN_4O_{12}S_2 \cdot 1.5H_2O$ (955.55): C, 52.79; H, 5.38; N, 5.86%. Found: C, 52.72; H, 5.53; N, 5.88%. FAB MS(+) $m/z = 583.7$ (584.17 calcd for $CuL^a + H^+$); IR (KBr): 1627 cm^{-1} ($\nu_{C=N}$), 1035, 1011, 817, 684, 569 cm^{-1} (TsO$^-$).

ZnL^a·2TsOH: Yellowish brown solid (0.70 g, 75%). Mp >220 °C (decomp.); Anal. Calcd for $C_{42}H_{48}N_4O_{12}S_2Zn \cdot H_2O$ (948.39): C, 53.19; H, 5.31; N, 5.91%. Found: C, 53.04; H, 5.37; N, 5.75%. FAB MS(+) $m/z = 585.2$ (586.97 calcd for $ZnL^a + H^+$); IR (KBr): 1617 cm^{-1} ($\nu_{C=N}$), 1035, 1011, 817, 686, 570 cm^{-1} (TsO$^-$); ^{1}H NMR: δ 2.28 (s, ArH, 6H), 2.31 (s, TsH, 6H), 2.74 (s, N–CH$_3$, 12H), 4.12 (s, –CH$_2$–, 4H), 6.97 (s, ArH, 2H), 7.10 (d, $^3J = 7.9$ Hz, TsH, 4H), 7.47 (d, $^3J = 7.9$ Hz, TsH, 4H), 7.65 (s, ArH, 2H), 7.86 (brs, –OH, 2H), 8.88 (s, –N=CH–, 2H), 9.0 (br, –NH, 2H), 9.8 (br, –OH, 2H); ^{13}C NMR: δ 19.6, 20.8, 41.9, 105.8, 112.4, 125.5, 125.6, 128.2, 135.4, 135.7, 136.9, 137.9, 145.5, 145.4, 161.6.

Synthesis of Divalent Metal Complexes of L^b (ML^b; M = Ni, Cu, Zn). To a THF solution (10 mL) of $\mathbf{H_2L^b}$ (0.41 g, 1 mmol) was added a methanol solution (10 mL) of the corresponding metal acetate hydrate (1 mmol). Within several hours the mixture gave a precipitate, which was collected by filtration and washed with methanol.

NiL^b: Reddish brown solid (0.41 g, 89%). Mp >300 °C (decomp.); Anal. Calcd for $C_{22}H_{18}N_2NiO_6 \cdot H_2O$ (483.10): C, 54.70; H, 4.17; N, 5.80%. Found: C, 54.78; H, 4.01; N, 5.77%. FAB MS(+) $m/z = 465.0$ (465.05 calcd for $NiL^b + H^+$); IR (KBr): 1626 cm^{-1} ($\nu_{C=N}$); ^{1}H NMR: δ 2.24 (s, –CH$_3$, 6H), 6.26 (d, $^3J = 8.8$ Hz, ArH, 2H), 6.90 (d, $^3J = 8.8$ Hz, ArH, 2H), 7.79 (s, ArH, 2H), 8.06 (brs, –OH, 2H), 8.47 (s, –N=CH–, 2H), 9.36 (brs, –OH, 2H); ^{13}C NMR spectrum has not been obtained due to insufficient solubility.

CuL^b: Reddish brown solid (0.41 g, 87%). Mp >300 °C (decomp.); Anal. Calcd for $C_{22}H_{18}CuN_2O_6 \cdot 0.5H_2O$ (478.94): C, 55.17; H, 4.00; N, 5.85%. Found: C, 54.78; H, 3.79; N, 5.72%. FAB MS(+) $m/z = 470.1$ (470.05 calcd for $CuL^b + H^+$), IR (KBr): 1620 cm^{-1} ($\nu_{C=N}$).

ZnL^b: Yellowish brown solid (0.46 g, 97%). Mp >300 °C (decomp.); Anal. Calcd for $C_{22}H_{18}N_2ZnO_6 \cdot 1.5H_2O$ (498.80): C, 52.97; H, 4.24; N, 5.62%. Found: C, 53.35; H, 4.01; N, 5.60%. FAB MS(+) $m/z = 471.1$ (471.05 calcd for $ZnL^b + H^+$); IR (KBr): 1618 cm^{-1} ($\nu_{C=N}$); ^{1}H NMR: δ 2.29 (s, –CH$_3$, 6H), 6.13 (d, $^3J = 9.0$ Hz, ArH, 2H), 6.77 (d, $^3J = 9.0$ Hz, ArH, 2H), 7.56 (brs, –OH, 2H), 7.63 (s, ArH, 2H), 8.84 (s, –N=CH–, 2H), 9.13 (brs, –OH, 2H); ^{13}C NMR: δ 19.5, 105.4, 112.6, 116.5, 125.9, 135.1, 135.2, 136.9, 147.2, 160.3, 160.8.

Crystallography. For X-ray diffraction of single crystals, data were collected on a MacScience DIP Labo Imaging Plate diffractometer, $\mu(\mathrm{Cu\,K}\alpha) = 1.5418$ Å. The structure was solved by direct methods and expanded using Fourier techniques. All calculations were performed with the crystallographic software package SHELX-97.[39] Crystallographic data have been deposited with Cambridge Crystallographic Data Centre: Deposition numbers CCDC-900253 to compound $\mathbf{1H_3}$. Copies of the data can be obtained free of charge via http://www.ccdc.cam.ac.uk/conts/retrieving.html (or from the Cambridge Crystallographic Data Centre, 12, Union Road, Cambridge, CB2 1EZ, U.K.; Fax: +44 1223 336033; e-mail: deposit@ccdc.cam.ac.uk).

Crystal Data of $\mathbf{1H_3}$: $(C_{10}H_{13}NO_4)_2 \cdot 0.5H_2O$, colorless plate, $M_r = 215.72$, monoclinic, $a = 9.5940(3)$, $b = 12.1230(4)$, $c = 18.3890(6)$ Å, $\beta = 92.511(2)°$, $V = 2136.74(12)$ Å^3, $D_{\mathrm{calcd}} = 1.341$ g cm^{-3}, $T = 193$ K, space group $P2/n$ (#13), $Z = 4$, $\mu(\mathrm{Cu\,K}\alpha) = 8.88$ cm^{-1}, 19461 reflections measured and 3450 unique ($2\theta_{\max} = 144.1°$, $R_{\mathrm{int}} = 0.034$) which were used in all calculations. $R = 0.073$, $R_w = 0.196$.

The authors are grateful to Prof. Kazuyuki Ishii at the University of Tokyo and Dr. Atsushi Okazawa at the University of Tokyo for their kind cooperation on ESR measurements and helpful discussion about organic radicals.

Supporting Information

Supplementary spectra, crystallograms, voltammograms, and computational data. This material is available free of charge on the Web at: http://www.csj.jp/journals/bcsj/.

References

1 J. Stubbe, D. G. Nocera, C. S. Yee, M. C. Y. Chang, *Chem. Rev.* **2003**, *103*, 2167.

2 J. W. Whittaker, *Chem. Rev.* **2003**, *103*, 2347.

3 a) M. M. Whittaker, P. J. Kersten, N. Nakamura, J. Sanders-Loehr, E. S. Schweizer, J. W. Whittaker, *J. Biol. Chem.* **1996**, *271*, 681. b) M. M. Whittaker, P. J. Kersten, D. Cullen, J. W. Whittaker, *J. Biol. Chem.* **1999**, *274*, 36226.

4 S. Itoh, M. Taki, S. Fukuzumi, *Coord. Chem. Rev.* **2000**, *198*, 3.

5 B. A. Jazdzewski, W. B. Tolman, *Coord. Chem. Rev.* **2000**, *200–202*, 633.

6 W. Kaim, *Dalton Trans.* **2003**, 761.

7 a) D. Parker, E. S. Davies, C. Wilson, J. McMaster, *Inorg. Chim. Acta* **2007**, *360*, 203. b) L. Benisvy, A. J. Blake, D. Collison, E. S. Davies, C. D. Garner, E. J. L. McInnes, J. McMaster, G. Whittaker, C. Wilson, *Dalton Trans.* **2003**, 1975. c) L. Benisvy, E. Bill, A. J. Blake, D. Collison, E. S. Davies, C. D. Garner, G. McArdle, E. J. L. McInnes, J. McMaster, S. H. K. Ross, C. Wilson, *Dalton Trans.* **2006**, 258. d) L. Benisvy, E. Bill, A. J. Blake, D. Collison, E. S. Davies, C. D. Garner, C. I. Guindy, E. J. L. McInnes, G. McArdle, J. McMaster, C. Wilson, J. Wolowska, *Dalton Trans.* **2004**, 3647.

8 A. Mukherjee, F. Lloret, R. Mukherjee, *Eur. J. Inorg. Chem.* **2010**, 1032.

9 J. Müller, A. Kikuchi, E. Bill, T. Weyhermüller, P. Hildebrandt, L. Ould-Moussa, K. Wieghardt, *Inorg. Chim. Acta* **2000**, *297*, 265.

10 C. G. Pierpont, *Coord. Chem. Rev.* **2001**, *216–217*, 99.

11 P. Chaudhuri, C. N. Verani, E. Bill, E. Bothe, T. Weyhermüller, K. Wieghardt, *J. Am. Chem. Soc.* **2001**, *123*, 2213.

12 E. Evangelio, D. Ruiz-Molina, *Eur. J. Inorg. Chem.* **2005**, 2957.

13 P. Gütlich, Y. Garcia, T. Woike, *Coord. Chem. Rev.* **2001**, *219–221*, 839.

14 O. Margeat, P. G. Lacroix, J. P. Costes, B. Donnadieu, C. Lepetit, K. Nakatani, *Inorg. Chem.* **2004**, *43*, 4743.

15 T. J. O'Sullivan, B. Djukic, P. A. Dube, M. T. Lemaire, *Chem. Commun.* **2009**, 1903.

16 D. Kiriya, H.-C. Chang, K. Nakamura, D. Tanaka, K. Yoneda, S. Kitagawa, *Chem. Mater.* **2009**, *21*, 1980.

17 a) O. Rotthaus, F. Thomas, O. Jarjayes, C. Philouze, E. Saint-Aman, J.-L. Pierre, *Chem.—Eur. J.* **2006**, *12*, 6953. b) O. Rotthaus, O. Jarjayes, F. Thomas, C. Philouze, E. Saint-Aman, J.-L. Pierre, *Dalton Trans.* **2007**, 889. c) O. Rotthaus, O. Jarjayes, C. Philouze, C. P. Del Valle, F. Thomas, *Dalton Trans.* **2009**, 1792. d) H. Arora, C. Philouze, O. Jarjayes, F. Thomas, *Dalton Trans.* **2010**, *39*, 10088.

18 a) Y. Shimazaki, F. Tani, K. Fukui, Y. Naruta, O. Yamauchi, *J. Am. Chem. Soc.* **2003**, *125*, 10512. b) Y. Shimazaki, T. Yajima, F. Tani, S. Karasawa, K. Fukui, Y. Naruta, O. Yamauchi, *J. Am. Chem. Soc.* **2007**, *129*, 2559. c) Y. Shimazaki, N. Arai, T. J. Dunn, T. Yajima, F. Tani, C. F. Ramogida, T. Storr, *Dalton Trans.* **2011**, *40*, 2469.

19 T. J. Dunn, C. F. Ramogida, C. Simmonds, A. Paterson, E. W. Y. Wong, L. Chiang, Y. Shimazaki, T. Storr, *Inorg. Chem.* **2011**, *50*, 6746.

20 A. Kochem, O. Jarjayes, B. Baptiste, C. Philouze, H. Vezin, K. Tsukidate, F. Tani, M. Orio, Y. Shimazaki, F. Thomas, *Chem.—Eur. J.* **2012**, *18*, 1068.

21 a) S. Routier, H. Vezin, E. Lamour, J.-L. Bernier, J.-P.

Catteau, C. Bailly, *Nucleic Acids Res.* **1999**, *27*, 4160. b) E. Lamour, S. Routier, J.-L. Bernier, J.-P. Catteau, C. Bailly, H. Vezin, *J. Am. Chem. Soc.* **1999**, *121*, 1862. c) H. Vezin, E. Lamour, S. Routier, F. Villain, C. Bailly, J.-L. Bernier, J. P. Catteau, *J. Inorg. Biochem.* **2002**, *92*, 177.

22 S. S. Tonde, A. S. Kumbhar, S. B. Padhye, R. J. Butcher, *J. Inorg. Biochem.* **2006**, *100*, 51.

23 S. J. Wezenberg, A. W. Kleij, *Angew. Chem., Int. Ed.* **2008**, *47*, 2354.

24 S. Akine, *J. Inclusion Phenom. Macrocyclic Chem.* **2012**, *72*, 25.

25 A. C. W. Leung, M. J. MacLachlan, *J. Inorg. Organomet. Polym. Mater.* **2007**, *17*, 57.

26 S. Akine, T. Nabeshima, *Dalton Trans.* **2009**, 10395.

27 J. Jiang, M. J. MacLachlan, *Chem. Commun.* **2009**, 5695.

28 M. Narita, I. Yoon, M. Aoyagi, M. Goto, T. Shimizu, M. Asakawa, *Eur. J. Inorg. Chem.* **2007**, 4229.

29 a) T. F. Markle, I. J. Rhile, A. G. DiPasquale, J. M. Mayer, *Proc. Natl. Acad. Sci. U.S.A.* **2008**, *105*, 8185. b) I. J. Rhile, T. F. Markle, H. Nagao, A. G. DiPasquale, O. P. Lam, M. A. Lockwood, K. Rotter, J. M. Mayer, *J. Am. Chem. Soc.* **2006**, *128*, 6075.

30 J. L. Dempsey, J. R. Winkler, H. B. Gray, *Chem. Rev.* **2010**, *110*, 7024.

31 F. Thomas, H. Arora, C. Philouze, O. Jarjayes, *Inorg. Chim. Acta* **2010**, *363*, 3122.

32 S. W. Ng, *Acta Crystallogr., Sect. E: Struct. Rep. Online* **2008**, *64*, o1565.

33 J. Kruszewski, T. M. Krygowski, *Tetrahedron Lett.* **1972**, *13*, 3839.

34 H. Houjou, T. Motoyama, S. Banno, I. Yoshikawa, K. Araki, *J. Org. Chem.* **2009**, *74*, 520.

35 T. Maki, Y. Araki, Y. Ishida, O. Onomura, Y. Matsumura, *J. Am. Chem. Soc.* **2001**, *123*, 3371.

36 F. Thomas, O. Jarjayes, H. Jamet, S. Hamman, E. Saint-Aman, C. Duboc, J.-L. Pierre, *Angew. Chem., Int. Ed.* **2004**, *43*, 594.

37 E. R. Altwicker, *Chem. Rev.* **1967**, *67*, 475.

38 a) H. Houjou, T. Motoyama, K. Araki, *Eur. J. Inorg. Chem.* **2009**, 533. b) H. Houjou, M. Ito, K. Araki, *Inorg. Chem.* **2009**, *48*, 10703. c) H. Houjou, M. Ito, K. Araki, *Inorg. Chem.* **2011**, *50*, 5298.

39 G. M. Sheldrick, *Acta Crystallogr., Sect. A: Found. Crystallogr.* **2008**, *64*, 112.